Pigs are highly susceptible to but do not transmit mink-derived highly pathogenic avian influenza virus H5N1 clade 2.3.4.4b

Taeyong Kwon[1], Jessie D. Trujillo[1], Mariano Carossino[2], Eu Lim Lyoo[1], Chester D. McDowell[1], Konner Cool[1], Franco S. Matias-Ferreyra[1], Trushar Jeevan[3], Igor Morozov[1], Natasha N. Gaudreault[1], Udeni B.R. Balasuriya[2], Richard J. Webby[3], Nikolaus Osterrieder[1,4], Juergen A. Richt[1,*]

1 Department of Diagnostic Medicine/Pathobiology, College of Veterinary Medicine, Kansas State University, Manhattan, KS, USA

2 Louisiana Animal Disease Diagnostic Laboratory and Department of Pathobiological Sciences, School of Veterinary Medicine, Louisiana State University, Baton Rouge, LA, USA

3 Department of Infectious Diseases, St. Jude Children's Research Hospital, Memphis, TN, USA

4 Institut für Virologie, Freie Universität Berlin, Berlin, Germany

[*] Corresponding author: Dr. Juergen A. Richt; e-mail: jricht@ksu.edu

Abstract

Rapid evolution of highly pathogenic avian influenza viruses (HPAIVs) is driven by antigenic drift but also by reassortment, which might result in robust replication in and transmission to mammals. Recently, spillover of clade 2.3.4.4b HPAIV to mammals including humans, and their transmission between mammal species has been reported. This study aimed to evaluate the pathogenicity and transmissibility of a mink-derived clade 2.3.4.4b H5N1 HPAIV isolate from Spain in pigs. Experimental infection caused moderate to severe interstitial pneumonia with necrotizing bronchiolitis with high titers of virus present in the lower respiratory tract of principal-infected pigs and 100% seroconversion. Principal-infected pigs shed limited amount of virus through the nasal and oral cavities, and importantly, there was no transmission to contact sentinel pigs. Notably, critical mammalian-like mutations such as PB2-E627K and HA-Q222L emerged at low frequencies in clinical samples and tissues derived from principal-infected pigs. It is concluded that pigs are highly susceptible to infection with the mink-derived clade 2.3.4.4b H5N1 HPAIV and provide a favorable environment for HPAI viruses to acquire mammalian-like adaptations. This work is critical for further risk assessment on the ability of the newly emerging H5N1 clade 2.3.4.4b HPAIVs to cross the species barriers into mammals.

35 **Introduction**

36 Influenza A viruses (IAV) are members of the *Orthomyxoviridae*, family that encompasses single-
37 stranded, negative-sense, segmented RNA viruses. IAVs are classified into different subtypes based on the
38 two major surface proteins: hemagglutinin (HA) and neuraminidase (NA). Wild aquatic birds are natural
39 hosts for most IAV types, except for H17N10 and H18N11, which were first isolated from bats and seem
40 endemic in multiple bat species [1,2]. Highly pathogenic avian influenza (HPAI) viruses arise from the
41 evolution of low pathogenic avian influenza (LPAI) viruses by insertion of a stretch of basic amino acids
42 into the HA cleavage site, which enables efficient HA activation by ubiquitous cellular, furin-like
43 proteases; they cause systemic, lethal infections in poultry [3].

44 Since the first detection of HPAI H5 subtype viruses with the isolation of the A/Goose/Guangdong/1/1996
45 (GsGD) H5N1 virus in southern China in 1996, this lineage has genetically evolved and spread
46 worldwide primarily by migratory birds [4]. Continuous evolution of the GsGD-like H5 HPAI viruses lead
47 to the emergence of genetically distinct clades, and reassortment with other clades of HPAI viruses or
48 local LPAI viruses has resulted in remarkable genetic diversification through the acquisition of novel gene
49 segments [5]. Eventually, HPAI H5N1 clade 2 viruses became dominant and their descendants have been
50 responsible for subsequent HPAI outbreaks. One remarkable HPAI outbreak in North America happened
51 in 2014/2015, when Asian-origin HPAI H5 clade 2.3.4.4 viruses spread to North America via the Pacific
52 flyway (Alaska, Western Canada/USA) with migratory wild birds and underwent reassortment with local
53 North American LPAIVs, resulting in HPAI H5 viruses with multiple NA subtypes, including H5N1,
54 H5N2, H5N5, H5N6, and H5N8, collectively called H5Nx viruses [6]. The geographic expansion of the
55 H5Nx HPAI viruses via wild birds and increased virus molecular evolution resulted in the emergence and
56 dominance of H5 subtype clade 2.3.4.4b viruses which contributed to the H5N8 outbreaks in 2016/17
57 and 2020/21 and the H5N1 outbreaks in 2021/22 [7]. By 2021/22, H5N1 clade 2.3.4.4b infections had
58 caused massive HPAI outbreaks in Europe with subsequent spread to North America via Iceland and the
59 trans-Atlantic flyways [8].

60 The normal distribution of the receptors for avian and mammalian IAVs in the human respiratory tract
61 usually prevents efficient direct transmission of avian influenza viruses to humans, since the respective
62 avian-like receptor (sialic acid linked to galactose by an alpha-2,3 linkage) is found only on cells in the
63 lower respiratory tract region [9]. Nonetheless, in certain instances the human-animal interface allows avian
64 influenza viruses to cross species barriers and infect humans. Human infection with avian influenza
65 viruses occurs sporadically and results in mild to severe illness with a wide range of clinical symptoms.
66 Specifically, it has been reported that human infections with avian H5 and H7 subtype viruses can cause
67 severe illness in humans with case fatality rates of 52% and 39%, respectively [10]. Human infections with
68 HPAI H5N1 viruses have been attributed to direct exposure to infected poultry or infected wild birds.
69 Importantly, the current epidemiological data do not provide evidence for sustained human-to-human
70 transmission of HPAI H5 viruses [11]. Since the beginning of 2020, human infections with clade 2.3.4.4b
71 H5N1 have been documented in China, Spain, UK, USA, and Vietnam, and all cases were linked to close
72 contact with infected poultry [12]. In addition, the ability of the clade 2.3.4.4b H5N1 viruses to cross the
73 species barrier is clearly supported by its detection in a variety of mammalian species such as terrestrial
74 and marine mammals [12]. In October 2022, an outbreak of the clade 2.3.4.4b H5N1 HPAI virus in farmed
75 mink in Spain was reported, with clear evidence of sustained mink-to-mink transmission [13], raising
76 concerns about the adaptation of the clade 2.2.4.4b H5N1 virus to mammals. Therefore, in order to
77 determine the risk of the mink-derived clade 2.3.4.4b H5N1 virus isolate, this study evaluated its
78 virulence and transmissibility in pigs, which are natural hosts for IAVs and the "mixing vessel" for the
79 reassortment and establishment of potentially pandemic influenza viruses.

80

81 **Materials and Methods**

82 **Cells and virus**

83 Madin-Darby canine kidney (MDCK) cells were maintained in Dulbecco's Modified Eagle Medium
84 (DMEM; Corning, Manassas, VA, USA) supplemented with 5% fetal bovine serum (FBS; R&D systems,
85 Flower Branch, GA, USA) and a 1% antibiotic-antimycotic solution (Gibco, Grand Island, NY, USA).
86 The mink-derived clade 2.3.4.4b H5N1 isolate, A/Mink/Spain/3691-8_22VIR10586-10/2022, was kindly
87 provided by Francesco Bonfante and Isabella Monne from the Istituto Zooprofilattico Sperimentale delle
88 Venezie, Legnaro, Italy, and Monserrat Agüero and Azucena Sánchez from the Laboratorio Central
89 Veterinario (LCV), Ministry of Agriculture, Fisheries and Food, Madrid, Spain, via Dr. Richard Webby
90 from St. Jude Childrens' Research Hospital, Memphis, TN.

91 **Pig infection experiment**

92 Fifteen 4-week-old piglets were obtained from a high health status pig herd at Kansas State University.
93 The pigs were separated into two groups: a principal-infected group and a sentinel group that were housed
94 in separate pens. Nine pigs were challenged with a total dose of 2.2×10^7 $TCID_{50}$ in 4 mL of DMEM: 1
95 mL orally, 1mL intranasally, and 2 mL intratracheally (see Figure 1A). On day 2 after infection, principal-
96 infected and sentinel pigs were co-mingled and co-housed in a single pen. Nasal swab samples were
97 collected in 2 mL of DMEM containing 1X antibiotic/antimycotic solution at -1, 1 to 14, 17, and 21 days
98 post-challenge (DPC), oropharyngeal swabs on days -1, 1, 3, 5, 7, 10, 14, 17, and 21 DPC. Three of the
99 principal-infected pigs each were euthanized and necropsied at 3 and 5 DPC, and the remaining 3
100 principal and 6 sentinel pigs were euthanized and necropsied at 21 DPC. At necropsy, gross pathology
101 evaluation was performed (see below) and bronchoalveolar lavage fluid (BALF) and tissue samples were
102 collected for virological and histopathological evaluation.

103 **Virus isolation**

104 MDCK cells were used to isolate the virus from clinical samples, which were filtered through a 0.45 µm
105 syringe filter except for BALF. Ten-fold serial dilutions of samples were prepared and transferred on
106 confluent MDCK cells after washing with PBS. The plates were subjected to immunofluorescence assay

107 (IFA) on day 2. Briefly, the cells were fixed with ice-cold methanol and incubated with the HB65
108 monoclonal antibody targeting the IAV nucleoprotein [14]. After washing, the cells were incubated with
109 anti-mouse conjugated with Alexa Fluor 488 (Invitrogen, Carlsbad, CA, USA). Virus titers were
110 calculated using the Reed-Muench method [15].

111 **RNA extraction and M gene-specific RT-qPCR**

112 Viral RNA was extracted using a magnetic bead-based automated extraction system (Taco Mini and total
113 nucleic acid extraction kit, Gene Reach, USA) [16]. Briefly, the swabs, BALF samples and 10% tissue
114 homogenates were mixed with an equal volume of the RLT buffer (Qiagen, Germantown, MD, USA).
115 Two hundreds microliter of the sample lysate and 200 μL isopropanol was added into the extraction plate.
116 RT-qPCR was performed using the previously published primers and the modified probe (A to G at 66) in
117 qScript XLT 1-Step RT-qPCR ToughMix (QuantaBio, Beverly, MA, USA) [17].

118 **Serology**

119 Virus neutralization tests were performed according to a previously established protocol [18]. Briefly, equal
120 volumes of heat-treated serum (50 μL) and 100 $TCID_{50}$/50 μL of virus were mixed and incubated at 37°C
121 for 1 hour. The mixture was transferred onto pre-washed MDCK cells. On day 2, IFA was performed to
122 determine 50% inhibition of virus growth. In addition, commercially available enzyme-linked
123 immunosorbent assay (ELISA) kits were used to evaluate the antibody responses according to the
124 manufacturers' instruction: (1) ID Screen® Influenza A Nucleoprotein Swine Indirect, Innovative
125 Diagnostics, France, (2) ID Screen® Influenza A Antibody Competition Multi-Species, Innovative
126 Diagnostics, France, and (3) IDEXX AI MultiS-Screen Ab Test, IDEXX, USA.

127 **Gross pathology and histopathology**

128 *Post-mortem* examinations were conducted at 3, 5, and 21 DPC. Macroscopic pathology was scored *in*
129 *toto*, and the percentage of lung lesions calculated based on the previous published method protocols [19].
130 Tissue samples were fixed in 10% neutral buffered formalin, processed, and stained with hematoxylin and

131 eosin (H&E). Microscopic pathology was evaluated based on microanatomy of the lung using previously
132 described scoring scale with minor modifications [20]. Each lung section was scored from 0 to 4 scale (0=
133 absent, 1=minimal, 2=mild, 3=moderate, and 4=severe) for six separate criteria typically associated with
134 influenza A virus infections in pigs: (i) epithelial necrosis, attenuation or disruption; (ii) airway exudate;
135 (iii) percentage of airways with inflammation; (iv) peribronchiolar and perivascular lymphocytic
136 inflammation; (v) alveolar exudate; (vi) alveolar septal inflammation. For scoring the percentage of
137 airways with inflammation (iii): 0%=0, up to 10% involvement =1, 10–39% involvement =2, 40–69%
138 involvement =3 and, greater than 70% involvement =4.

139 **Influenza A virus-specific immunohistochemistry (IHC)**

140 Immunohistochemistry (IHC) for detection of Influenza virus A H5N1 nucleoprotein (NP) antigen was
141 performed on the automated BOND RXm platform and the Polymer Refine Red Detection kit (Leica
142 Biosystems, Buffalo Grove, IL). Following automated deparaffinization, four-micron formalin-fixed,
143 paraffin-embedded tissue sections on positively charged Superfrost® Plus slides (VWR, Radnor, PA)
144 were subjected to automated heat-induced epitope retrieval (HIER) using a ready-to-use EDTA-based
145 retrieval solution (pH 9.0, Leica Biosystems) at 100 °C for 20 min. Subsequently, tissue sections were
146 incubated with the primary antibody (rabbit polyclonal anti-Influenza A virus NP [ThermoFisher
147 Scientific, PA5-32242] diluted 1:500 in Primary Antibody diluent [Leica Biosystems]) for 30 min at
148 ambient temperature followed by a polymer-labeled goat anti-rabbit IgG coupled with alkaline
149 phosphatase (30 min). Fast Red was used as the chromogen (15 min), and counterstaining was performed
150 with hematoxylin for 5 min. Slides were dried in a 60 °C oven for 30 min and mounted with a permanent
151 mounting medium (Micromount®, Leica Biosystems). Lung sections from a pig experimentally infected
152 with swine influenza virus A/swine/Texas/4199-2/1998 H3N2 were used as a positive assay control.

153 **Influenza A virus H5N1 mink-specific RNAscope® in situ hybridization.**

154 For RNAscope® in situ hybridization (ISH), an anti-sense probe targeting the NP and the hemagglutinin
155 (HA [H5 subtype]) of influenza virus A/Mink/Spain/3691-8_22VIR10586-10/2022 clade 2.3.4.4b
156 (GISAID # EPI_ISL_15878539) were designed (Advanced Cell Diagnostics (ACD), Newark, CA, USA).
157 Sections of formalin-fixed paraffin-embedded tissues were generated as indicated above, and the
158 RNAscope® ISH assay was performed using the RNAscope 2.5 LSx Reagent Kit (ACD) on the
159 automated BOND RXm platform (Leica Biosystems, Buffalo Grove, IL, USA). Following automated
160 baking and deparaffinization, tissue sections were subjected to heat-induced epitope retrieval (HIER)
161 using an EDTA-based solution (pH 9.0; Leica Biosystems) at 100°C for 15 min, protease digestion using
162 the RNAscope® 2.5 LSx Protease for 15 min at 40 °C, and incubation with a ready-to-use hydrogen
163 peroxide solution for 10 min at room temperature. Slides were incubated with each probe mixture for 2 h
164 at 40 °C, and the signal was amplified using a specific set of amplifiers (AMP1 through AMP6) as
165 recommended by the manufacturer. The signal was detected using a Fast-Red solution for 10 min at room
166 temperature. Slides were counterstained with a ready-to-use hematoxylin for 5 min, followed by five
167 washes with 1X BOND Wash Solution (Leica Biosystems). Slides were finally rinsed in deionized water,
168 dried in a 60 °C oven for 30 min, and mounted with Ecomount® (Biocare, Concord, CA, USA). Lung
169 sections from a pig experimentally infected with swine influenza virus A/swine/Texas/4199-2/1998 H3N2
170 were used as a positive assay control for the NP-specific probe, while lung sections from this study were
171 used in conjunction with the former to validate the HA-specific probe.

172 **Next-generation sequencing (NGS)**

173 The whole genome sequence of the mink-derived H5N1 clade 2.3.4.4b virus was determined using the
174 Illumina MiSeq sequencing platform (Illumina, San Diego, CA, USA). Briefly, viral RNA was extracted
175 from the challenge virus inoculum and virus-positive clinical samples using the QIAamp viral RNA mini
176 kit (Qiagen, Germantown, MD, USA) according to the manufacturer's instructions. Viral gene segments
177 were amplified using SuperScript™ III One-Step RT-PCR System with Platinum™ Taq DNA Polymerase
178 (Thermo Fisher Scientific, Waltham, WA, USA) with the Opti and Uni universal influenza primer sets [21,22]

179 or with SuperScript™ IV First-Strand Synthesis System and Platinum™ SuperFi™ DNA Polymerase
180 (Thermo Fisher Scientific, Waltham, WA, USA) with previously published segment specific primer sets
181 [23]. All samples were normalized to 100−500 ng of DNA prior to library preparations. Sequencing libraries
182 were prepared using the Illumina DNA Prep kit (Illumina, San Diego, CA). Libraries were sequenced
183 using pair-end chemistry on the Illumina MiSeq platform with the Miseq v2 Reagent kit (300 cycles).
184 Sequencing reads were demultiplexed and parsed into individual FASTQ files and imported into CLC
185 Genomics Workbench version 22.0.1 (Qiagen, Germantown, MD, USA) for analysis. Reads were
186 trimmed to remove primer sequences and filtered to remove low quality and short reads. The trimmed
187 reads were mapped to the reference sequences (GISAID accession numbers: EPI2220590 to
188 EPI2220597). Following read mapping, all samples were run through the low frequency variant caller
189 module within CLC Genomic Workbench with a frequency cutoff greater than 2%.

190

191 **Results**

192 **Infection of pigs with the mink-derived clade 2.3.4.4b H5N1**

193 This study aimed to elucidate the pathogenicity and transmissibility of the mink-derived clade 2.3.4.4b
194 H5N1 virus in pigs. At 24 hours post-challenge, all principal-infected pigs became lethargic, and five of
195 nine pigs were febrile with average temperatures of 41 °C. However, the average temperature decreased
196 to 39.5 °C at 2 DPC and pigs were healthy with no obvious clinical signs throughout the rest of the
197 observation period (Supplementary Figure 1).

198 Infectious virus was isolated from nasal (6/9 animals positive) and oropharyngeal swabs (4/9 positive)
199 from principal infected pigs and the titers ranged from 4.46×10^1 to 1×10^3 $TCID_{50}$/mL at 1 DPC (Table
200 1). At 3 DPC, one nasal and one oropharyngeal swab were virus positive, with titers of 2.15×10^3 and
201 4.64×10^2 $TCID_{50}$/mL, respectively. Infectious virus was still present in the nasal swab at 5 DPC ($2.15 \times$
202 10^2 $TCID_{50}$/mL). RT-qPCR results showed that all principal-infected animals were positive on at least one

203 time point from 1–5 DPC in either the nasal or oropharyngeal swabs (Supplementary Figure 2A and 2B).
204 All swabs collected from sentinel pigs were negative by virus isolation and RT-qPCR throughout the
205 entire observation period.

206 To determine virus replication and distribution in tissues, virus titers were determined in BALF and
207 various tissue samples. All BALF samples at 3 and 5 DPC were positive with virus titers of 2.15×10^3 to
208 4.64×10^4 $TCID_{50}$/mL at 3 DPC and 4.64×10^2 to 3.16×10^3 $TCID_{50}$/mL at 5 DPC (Figure 1B).
209 Infectious virus could also be isolated from tracheas (3/6), bronchi (2/6), lung tissues (5/6),
210 tracheobronchial lymph nodes (1/6), and tonsils (1/6) of six principal-infected pigs that were euthanized
211 at 3 (n=3 pigs) and 5 (n=3 pigs) DPC (Figure 1C and 1D). Interestingly, viral RNA was detectable in the
212 ethmoturbinates of all three animals sacrificed at 3 DPC (Supplementary Figure 2C). In addition, viral
213 RNA was present in the nasal turbinate of one pig at 3 DPC; this pig shed infectious virus from the nasal
214 cavity at 1 and 3 DPC. In contrast, the brain and olfactory bulb at 3 and 5 DPC were negative as assessed
215 by virus isolation and RT-qPCR (Supplementary Figure 2C and 2D). As expected, BALF and tissue
216 samples from both principal-infected and sentinel animals at 21 DPC were negative by both virus
217 isolation and RT-qPCR.

218 To determine the antibody responses in principal-infected and sentinel pigs, virus neutralization tests
219 (VNTs) and enzyme-link immunosorbent assays (ELISAs) were performed. Neutralizing antibodies were
220 detectable in all three principal-infected animals starting at 7 DPC and all principals were sero-positive at
221 14 and 21 DPC (Figure 1E), with neutralization titers ranging from 1:10 to 1:160. The NP-based indirect
222 ELISA revealed that two out of three principal-infected animals seroconverted at 7 DPC, with the levels
223 of antibodies in all three principal-infected pigs against NP increasing by 14 and 21 DPC (Figure 1F).
224 Two different NP-based competitive ELISAs confirmed the seroconversion of the three principal-infected
225 pigs at the 14 and 21 DPC (Supplementary Figure 3A and 3B).

226 **Macroscopic and microscopic pathology**

227 At 3 DPC, moderate to severe, multifocal to coalescing interstitial pneumonia with marked congestion
228 and edema affected all lobes were noted in 2/3 euthanized animals, while the remaining animal had mild,
229 multifocal pneumonia with congestion predominately the right lung and left caudal lung lobes
230 (Supplementary Figure 4A–4C). Pulmonary lesions consisted of moderate to severe non-suppurative
231 interstitial pneumonia with necrotizing bronchitis/bronchiolitis affecting multiple bronchopulmonary
232 segments, predominantly the pulmonary parenchyma adjacent to terminal bronchioles. Affected
233 bronchopulmonary segments were characterized by degeneration, attenuation and necrosis of the
234 bronchiolar epithelium and intraluminal cell debris and degenerate neutrophils, as well as peribronchiolar
235 and perivascular histiocytic, neutrophilic and lymphocytic inflammation locally extending to and
236 expanding alveolar septa. Smaller bronchi and bronchioles were most commonly affected, and necrotizing
237 alveolitis was characterized by alveolar spaces that contain inflammatory cells, occasional fibrin and
238 necrotic cell debris; the epithelial lining was segmentally to partially denuded or lined by swollen
239 degenerate epithelium (Figure 3A). These microscopic changes correlated with intracytoplasmic and/or
240 intranuclear viral NP antigen frequently within bronchial/bronchiolar epithelial cells, and less frequently
241 within pneumocytes and alveolar macrophages (Figure 3B). Viral NP (as determined by NP-specific IHC)
242 and H5-specific M or HA RNA (as determined by RNAscope® ISH) were predominantly detected within
243 airway epithelia and intraluminal necrotic cell debris, and sporadically in inflammatory cells within the
244 bronchiolar lamina propria (Figure 4A and 4B). In 1/3 pigs (#839), there was localized suppurative and
245 erosive rhinitis affecting the olfactory region (Supplementary Figure 5A). Within the affected region, viral
246 antigen was detected in sporadic foci of the olfactory neuroepithelium (Supplementary Figure 5B). Larger
247 airways (segmental bronchi and trachea) were affected by mild, multifocal neutrophilic to
248 lymphohistiocytic bronchitis and tracheitis, with frequent bronchial but rare tracheal epithelial cells
249 containing viral antigen (Supplementary Figure 5C and 5D).

250 By 5 DPC, multifocal to coalescing areas of pulmonary consolidation were observed on all pigs
251 (Supplementary Figure 4D–4F). In 2/3 pigs, focally extensive pneumonia was accompanied by large air-

252 filled bullae formation in the left dorsal lobes. Microscopically, alterations were similar to but more
253 extensive than those at 3 DPC with intense inflammation affecting larger regions of the pulmonary
254 parenchyma, with frequent bronchial/bronchiolar involvement and locally extensive alveolar collapse and
255 consolidation (Figure 3C). Viral NP antigen and, less frequently, NP- and HA-specific RNA were detected
256 in alveolar macrophages and intraluminal cell debris (Figure 3D and 4C–4D). In addition, numerous
257 individuals and small clusters of epithelia on medium to large airways contain viral antigen. Microscopic
258 changes in the trachea were mild and characterized by neutrophilic and lymphohistiocytic tracheitis with
259 sporadic epithelial cell degeneration/necrosis and rare intracytoplasmic viral antigen (Supplementary
260 Figure 5E and 5F). Multifocal, mild suppurative to erosive rhinitis affecting rostral turbinates was
261 identified, although in lieu of intralesional viral antigen. On 21 DPC, multiple foci of mild
262 lymphohistiocytic interstitial pneumonia were noted, accompanied by bronchiolar epithelial hyperplasia
263 (repair) with very rare bronchiolar epithelial cells or proprial mononuclear cells containing viral antigen
264 (Figure 3E and 3F).

265 Interestingly, Influenza A virus NP-positive antigen presenting cells were common within
266 tracheobronchial lymph nodes, most abundant at 3 DPC (with an average of 10-20 cells per 200X field)
267 and gradually reducing in numbers through 21 DPC (Supplementary Figure 6). No other significant gross
268 or histologic lesions, or viral antigen were identified in other organs examined.

269 **Emergence of mammalian-like mutations in H5N1-infected pigs**

270 The whole-length genome of the H5N1 virus inoculum, two nasal swabs, five oropharyngeal swabs and
271 six BALF samples were genetically characterized to determine genetic evolution of the H5N1 virus after
272 replication for up to 5 days in pigs. Our results show that the original mammalian-like PB2 T271A
273 mutation present in the inoculum remained stable with a frequency below 2% with no evidence of a
274 change in mutational frequency after virus replication for several days pigs (Table 2 and Supplementary
275 Table 2). Amino acid substitutions with a significant frequency (>2%) were found throughout all eight
276 viral segments in clinical samples from H5N1-infected pigs; these mutations were below a frequency of

277 2% in the virus inoculum (Supplementary Table 2). NGS analysis revealed that oropharyngeal swab #517
278 on 1 DPC had the mammalian-like K526R mutation of PB2 at a frequency of approximately 3% (Table
279 2). Interestingly, the critical mammalian adaptation mutations, PB2-E627K and PB2-E627V, were
280 identified in the oropharyngeal swab of pig #571 (E627K; 1 DPC) , the BALF sample of pig #839
281 (E627K; 3 DPC), in the oropharyngeal swab of pig #94 (E627V; 1 DPC) and the BALF sample of pig
282 #213 (E627V; 5 DPC) at a frequency of approximately 5%, 5%, 7% or 2%, respectively (see Table 2;
283 Supplementary Table 1). Furthermore, the oropharyngeal swab of pig #94 (1 DPC) had the Q222L
284 adaptation mutation in the HA gene at the frequency of 2.1%.

285

286 **Discussion**

287 Rapid evolution of IAV is driven by two mechanisms: (1) the introduction of point mutations by the error-
288 prone RNA polymerase, also called antigenic drift; and (2) by acquisition of one or more RNA segments
289 from another influenza virus, a process called reassortment or antigenic shift. Molecular evolution allows
290 IAVs to cross species barriers and acquire the ability to infect a wide range of hosts from avian species to
291 swine to humans. This broad host tropism provides opportunities for IAVs to gain distinct geno- and
292 phenotypes, to attain pandemic potential, and to evade pre-existing immunity in humans [24]. Specific host-
293 virus-environment characteristics accelerate the emergence of novel IAVs with pandemic potential. For
294 pandemic preparedness, it is critical to assess the potential pandemic risk of newly emerged IAVs; the
295 evaluation of certain virus characteristics is mainly done by *in vitro* and sometimes also *in vivo*
296 experiments [25]. However, it is essential to assess the pathogenesis and transmissibility of IAVs in target
297 animal models. Pigs are natural hosts for IAVs, and it is known that certain IAVs can be efficiently
298 transmitted between pigs. Importantly, interspecies transmissions between human and pigs and *vice versa*
299 are not uncommon and are facilitated by an extensive human-pig interface in various agricultural settings
300 [26]. Furthermore, pigs express receptors specific for both, mammalian and avian IAVs, providing
301 opportunities for co-infections with these viruses and the subsequent generation of novel reassortant

302 influenza viruses [27]. Recently, interspecies transmission of clade 2.3.4.4b H5N1 virus to mink and
303 sustained mink-to-mink transmission was reported in Spain, posing a significant concern to public health
304 [13]. Therefore, it was crucial to evaluate the pathogenicity and transmissibility of the recently emerged
305 clade 2.3.4.4b H5N1 virus isolated from diseased mink in domestic pigs.

306 One of key findings in this study was that experimental infection of pigs with the mink-derived clade
307 2.3.4.4b H5N1 virus resulted in productive virus replication and seroconversion in 100% of the principal-
308 infected pigs. Virus titers in BALF samples of principal-infected animals reached $10^{3.3}$ to $10^{4.7}$ $TCID_{50}$/mL
309 at 3 DPC and declined to $10^{2.7}$ to $10^{3.5}$ $TCID_{50}$/mL at 5 DPC. In addition, the virus was found in other
310 respiratory tissues, such as trachea, bronchi, as well as lymphoid tissues, such as tracheobronchial lymph
311 nodes and tonsils. Moreover, gross and histological evaluation of various tissues demonstrated that the
312 infection caused acute multifocal to coalescing necrotizing broncho-interstitial pneumonia at 3 and 5
313 DPC, with residual mild interstitial pneumonia still present at 21 DPC. Based on the microscopic lesion
314 distribution, virus titers and viral antigen/RNA tissue expression, it is clear that the lesions and
315 distribution of this mink-derived clade 2.3.4.4b H5N1 virus mostly involved the lower respiratory tract
316 (i.e., pulmonary parenchyma) with only mild alterations on the upper respiratory tract. Previous studies
317 demonstrated virus replication of avian-derived H5Nx clade 2.3.4.4 HPAI viruses from North America in
318 the lower respiratory tract of pigs upon experimental infection [28]. In the latter study, infection of pigs with
319 the avian-origin H5Nx clade 2.3.4.4 viruses, isolated in 2014 and 2015 in the U.S, led to viral RNA
320 detection in 80-100% of the animals and successful virus isolation in 60-100% of the BALF samples at 3
321 and 5 DPC [28]. Consistent with virus detection in the majority of animals, 60-100% of infected animals
322 seroconverted by 21 DPC (28). In addition, in a very recent study, low susceptibility of pigs against
323 experimental infection with an avian-derived H5N1 clade 2.3.4.4b virus, isolated from chickens in
324 Germany in 2022, was reported [29]. This chicken H5N1 clade 2.3.4.4b isolate lacked any mammalian-
325 adaptive mutations. Nasal and alimentary exposure of pigs to this avian-derived H5N21 clade 2.3.4.4b
326 virus only resulted in marginal virus replication, without inducing any clinical signs or pathological

327 changes. Only 1 out of 8 pigs seroconverted, indicating a rather high resistance of pigs to infection with
328 the avian-derived derived H5N21 clade 2.3.4.4b virus without mammalian-like adaptations [(29)].

329 Experimental infection of pigs with LPAI viruses without mammalian-like adaptations were also
330 previously performed, but none of the experimental infections with LPAI H5 viruses resulted in a
331 productive infection [30]. We conclude from our present study with the mink-derived clade 2.3.4.4b H5N1
332 HPAI virus, that this virus is not only able to efficiently infect mink, but also pigs. The mink-derived
333 H5N1 clade 2.3.4.4b virus efficiently replicated in the lower respiratory tract of pigs inducing sizeable
334 lung lesions; in addition, nasal and oral shedding was observed on early days after infection although less
335 efficient than reported for swine-derived influenza viruses [31,32]. However, it is important to note that the
336 mink-derived H5N1 clade 2.3.4.4b virus was unable to spread from principal-infected to co-mingled in-
337 contact sentinel animals; this was most likely due to the limited amount of virus shedding by the nasal
338 and oral cavities in principal-infected pigs. Interestingly, neither infectious virus, viral RNA nor
339 histopathological changes were present in tissues from the central nervous system of principal-infected
340 pigs in our study. In recent spillover events, wild mammals infected with the clade 2.3.4.4b H5N1 virus
341 primarily exhibited neurological symptoms with histopathological changes in brains as well as viral RNA
342 detection in CNS tissues [33-35]. Similarly, the mink infected with the H5N1 clade 2.3.4.4b virus used in this
343 study also showed neurological manifestations, such as ataxia and tremors [13]. We could not see any
344 neurological clinical signs in principal-infected pigs, indicating that the pathogenicity of the H5N1 clade
345 2.3.4.4b viruses could vary in different mammalian host species.

346 Earlier studies showed that experimental infection of pigs with avian-origin LPAI H5 subtype viruses
347 isolated between 1980 and 2005 led to nasal shedding of infectious virus of up to $10^{5.5}$ egg infectious
348 doses $(EID)_{50}$/mL and $10^{5.3}$ EID_{50}/100 mg [36,37]. In addition, it was shown that experimental infection of
349 pigs with human and avian-origin HPAI H5N1 viruses isolated in early (1997) and later (2004) in the
350 emergence of the HPAIV H5N1 resulted in the isolation of infectious virus in nasal swabs/nasal tracts
351 over the course of infection, but no pig-to-pig transmission [38,39]. When pigs were infected with the index

352 human H5N1 HPAIV strain (HK156-97) and an initial chicken H5N1 HPAIV isolate (CHK258-97) by the
353 oral and nasal routes, both the human and chicken H5N1 viruses replicated well in the nasal tract of pigs,
354 with the chicken isolate to higher titers than the human virus. Importantly, neither the human nor the
355 chicken H5N1 virus transmitted to contact pigs in the same pen. Thus, pigs support the replication of the
356 index human and an early chicken H5N1 virus to modest titers, and there was no detectable transmission
357 to contact animals [38]. Similarly, experimental studies on the replication and transmissibility of 2004 avian
358 H5N1 HPAI viruses associated with human infections in Vietnam to pigs revealed that H5N1 all viruses
359 tested replicated in the swine respiratory tract but none were transmitted to contact pigs (39).
360 Epidemiological studies showed limited serologic evidence (8/3175 pigs positive; 0.25%) of exposure to
361 the HPAI H5N1 viruses in Vietnamese pigs [39]. These findings indicate that pigs can be infected with the
362 2004 Vietnamese HPAI H5N1 viruses but that these viruses are not readily transmitted between pigs
363 under experimental conditions [39]. In contrast to the above described work, no viral RNA was detected in
364 nasal swabs of pigs infected with avian-derived clade 2.3.4.4 H5Nx viruses in 2014 [28], and only limited
365 detection of viral RNA but failure to isolate infectious virus was reported when pigs were infected with
366 an avian-derived clade 2.3.4.4b H5N1 virus without mammalian-like adaptations [29]. Collectively, these
367 results suggest that some isolates of HPAI H5 subtype viruses can replicate efficiently in the upper
368 respiratory tract of pigs, with limited replication in the lower respiratory tract. There is no transmission of
369 these viruses to co-mingled contact sentinels.

370 Through the continuous evolution of the HPAI H5Nx viruses over two decades, the
371 A/Goose/Guangdong/1/1996 H5N1 lineage (GsGD) may have acquired increased fitness in avian species
372 resulting in efficient spread across the globe. However, the continued adaptation of the H5N1 clade
373 2.3.4.4b virus to avian species may, in turn, contribute to a loss of fitness for mammalian species, which
374 resulted in its reduced replication capacity in the upper respiratory tract of pigs. Despite the shedding of
375 infectious virus in nasal and oropharyngeal secretions from principal-infected pigs, there was no evidence
376 of transmission of the mink-derived HPAI H5N1 clade 2.3.4.4b virus to sentinel pigs under our

377 experimental conditions. This result was consistent with previous findings indicating a lack of pig-to-pig
378 transmission for H5- or H7-subtype HPAIVs, regardless of the presence of infectious virus in nasal and/or
379 oral excretions [28,29,38,39]. The lack of transmissibility of the mink-derived H5N1 clade 2.3.4.4b isolate in
380 pigs is supported by the absence of seroconversion in the co-mingled sentinel animal; also, this virus did
381 not transmitted to the 11 farm workers that had been in close contact with the H5N1-infected minks at the
382 site of the outbreak [13]. Furthermore, a recent study showed that two other mink-derived H5N1 viruses
383 which differ by several amino acids in the PB2, PB1, PA, NA, NS1 and NS2 proteins, did not support
384 transmission to contact animals (neighboring cages) through respiratory droplets in the ferret model [40].
385 Importantly, it has been previously documented that H5 subtype viruses can acquire the ability to transmit
386 efficiently among pigs through reassortment. Lee *et al.* [41] isolated two H5N2 viruses from pigs showing
387 typical clinical symptoms of influenza-like illness; one was an avian-origin virus, the other one was an
388 avian-swine reassortant virus with PB2, PA, NP and M genes derived from swine influenza viruses. Upon
389 experimental infection of pigs, both viruses could be isolated from nasal swabs, but pig-to-pig
390 transmission occurred only in the group infected with the reassortant H5N2 virus [41].

391 One of the important findings is that the H5N1 viruses inoculated into pigs acquired mammalian-like
392 mutations/adaptations in the course of several days of pig infection, which potentially results in increased
393 fitness of the H5N1 virus in mammalian hosts. There is a total of four mink-derived H5N1 isolates from
394 the infected Spanish farm which were sequenced; all of them possessed the PB2 T271A mutation. The
395 PB2 T271A mutation is known to lead to enhanced polymerase activity in mammalian cells and might
396 have contributed to cross-species transmission from avian species to mammals including mink [13,42]. Our
397 results show that the T271A mutation was stable with no evidence of a change in the frequency of the
398 mutation after replication of the virus for several days in pigs. However, minor variants possessing the
399 mammalian-like E627K mutation in PB2 emerged in oropharyngeal swab (pig #714) and BALF (pig
400 #839) samples obtained from principal-infected pigs, even though they were found at low frequencies
401 (4.7% and 5.2%, respectively). The E627K mutation is a key determinant for mammalian adaptation of

402 avian influenza viruses; its introduction into the genome of an avian influenza virus enables efficient
403 replication of the avian-origin polymerase complex in mammalian cells [43]. It is well known that H5N1
404 viruses harboring the PB2 E627K mutation have increased virulence in mice; it also contributes to air-
405 borne virus transmission in ferrets and contact transmission in guinea pigs [44-48]. Similarly, an amino acid
406 substitution from glutamic acid (E) to valine (V) at position 627 of the PB2 gene (E627V) was shown to
407 increase viral replication in mammalian cells and virulence in mice models [49]; an E627V mutation was
408 detected as a minor virus population in the oropharyngeal swab of pig #94 and BALF sample of pig #213.
409 Furthermore, the oropharyngeal swab of gig #517 possessed a PB2 K526R mutation at the frequency of
410 3.1%; the K526R mutation was shown to enhance the effect of the PB2 E627K on avian influenza virus
411 replication in mammalian cells and also their virulence in mice [50]. Another key mutation is the Q222L
412 (according to the H5 numbering system) in the HA gene which is equivalent to a Q226L mutation using
413 the H3 numbering system. This mutation was found in oropharyngeal swab of pig #94 at 1 DPC. Amino
414 acid (AA) position 222 in the HA is involved in the binding of HA to its sialic acid receptor and plays a
415 critical role in determining the host range of IAVs. The HA of mammalian IAVs binds to α2,6-linked
416 sialic acid, whereas the HA of avian IAVs binds to α2,3-linked sialic acid. Several amino acids in the HA
417 receptor binding site are responsible for switching sialic acid specificity; however, the Q222L and G224S
418 AA positions in the H5 numbering system, which are equivalent to AA positions Q226L and G228S in the
419 H3 numbering system, are crucial for increased α2,6-sialic acid receptor preference in different subtypes
420 of avian IAVs; they are located in the receptor binding domain and interact directly with the host's sialic
421 acid receptor [51]. In addition, the Q222L mutation was previously described to contribute to the emergence
422 of transmissible H5N1 viruses via aerosols after serial passage of H5N1 in ferrets [45,46]. Despite the critical
423 role of these mutations in pathogenicity and transmissibility of IAVs in mammalian hosts, it still remains
424 unclear how the H5N1 clade 2.3.4.4b virus underwent its molecular evolution, and eventually acquired
425 critical mammalian-like mutations. In addition to the role of pigs in the ecology of IAVs as the "mixing
426 vessel", the emergence of mammalian-adapted H5N1 viruses in pigs is close to reality; therefore, pigs

427 may serve as the "hotspot" to introduce mammalian-like mutations into avian influenza viruses although
428 the frequencies of the mammalian-like mutations described here are rather low.

429 Spillover of H5N1 HPAI clade 2.3.4.4b viruses to mammals and their sustained transmission between
430 mammals has been reported [13,52]. The majority of mammals infected by the HPAI H5N1 clade 2.3.4.4b
431 virus are carnivores, and the consumption of infected dead wild birds is presumably the basis for these
432 spillover events [53]. In contrast to the HPAI H5N1 clade 2.3.4.4b virus infections in wild avians and wild
433 mammals, outbreaks in farmed avian and mammal species pose a much greater risk to humans, due to its
434 close proximity to occupational workers and -in the case of mammalian species - the favorable
435 environment for the acquisition of mammalian-like adaptations. Therefore, evaluating the
436 infectivity/susceptibility and transmissibility of the emerging HPAI viruses in well-established
437 mammalian animal models such as swine and ferrets is crucial to determine their pandemic potential. The
438 present study demonstrated that infection of pigs with the mink-derived clade 2.3.4.4b H5N1 virus led to
439 a productive viral replication in the respiratory tracts of all principal-infected pigs including
440 seroconversion; however, virus shedding from principal-infected pigs was not high and/or frequent
441 enough for an efficient transmission to co-mingled sentinel pigs. Notably, key mammalian-like
442 mutations were found in clinical and/or tissue samples derived from principal-infected pigs. In
443 conclusion, the results obtained in the present study suggest that the mink-derived H5N1 clade 2.3.4.4b
444 virus exhibited increased infectivity in pigs when compared to avian-origin H5N1 clade 2.3.4.4b viruses,
445 however, did not transmit to co-mingled sentinel animals; therefore, this virus would still be placed in a
446 moderate risk group in terms of transmission ability to humans.

447

448 **References**

449 1 Tong, S. *et al.* A distinct lineage of influenza A virus from bats. *Proc Natl Acad Sci U S A* **109**,
450 4269-4274 (2012). https://doi.org:10.1073/pnas.1116200109
451 2 Tong, S. *et al.* New world bats harbor diverse influenza A viruses. *PLoS Pathog* **9**, e1003657
452 (2013). https://doi.org:10.1371/journal.ppat.1003657

3 Vey, M. *et al.* Hemagglutinin activation of pathogenic avian influenza viruses of serotype H7 requires the protease recognition motif R-X-K/R-R. *Virology* **188**, 408-413 (1992). https://doi.org:10.1016/0042-6822(92)90775-k

4 Xu, X., Subbarao, Cox, N. J. & Guo, Y. Genetic characterization of the pathogenic influenza A/Goose/Guangdong/1/96 (H5N1) virus: similarity of its hemagglutinin gene to those of H5N1 viruses from the 1997 outbreaks in Hong Kong. *Virology* **261**, 15-19 (1999). https://doi.org:10.1006/viro.1999.9820

5 WHO/OIE/FAO H5N1 Evolution Working Group. Toward a unified nomenclature system for highly pathogenic avian influenza virus (H5N1). *Emerg Infect Dis* **14**, e1 (2008). https://doi.org:10.3201/eid1407.071681

6 World Health Organization. *Evolution of the influenza A(H5) haemagglutinin: WHO/OIE/FAO H5 Working Group reports a new clade designated 2.3.4.4*, <https://www.who.int/publications/m/item/evolution-of-the-influenza-a(h5)-haemagglutinin-who-oie-fao-h5-working-group-reports-a-new-clade-designated-2.3.4.4> (2015).

7 Pohlmann, A. *et al.* Has Epizootic Become Enzootic? Evidence for a Fundamental Change in the Infection Dynamics of Highly Pathogenic Avian Influenza in Europe, 2021. *mBio* **13**, e0060922 (2022). https://doi.org:10.1128/mbio.00609-22

8 Bevins, S. N. *et al.* Intercontinental Movement of Highly Pathogenic Avian Influenza A(H5N1) Clade 2.3.4.4 Virus to the United States, 2021. *Emerg Infect Dis* **28**, 1006-1011 (2022). https://doi.org:10.3201/eid2805.220318

9 Shinya, K. *et al.* Avian flu: influenza virus receptors in the human airway. *Nature* **440**, 435-436 (2006). https://doi.org:10.1038/440435a

10 World Health Organization. (2023).

11 Harfoot, R. & Webby, R. J. H5 influenza, a global update. *J Microbiol* **55**, 196-203 (2017). https://doi.org:10.1007/s12275-017-7062-7

12 World Health Organization. (2022).

13 Aguero, M. *et al.* Highly pathogenic avian influenza A(H5N1) virus infection in farmed minks, Spain, October 2022. *Euro Surveill* **28** (2023). https://doi.org:10.2807/1560-7917.ES.2023.28.3.2300001

14 Ma, W. *et al.* 2009 pandemic H1N1 influenza virus causes disease and upregulation of genes related to inflammatory and immune responses, cell death, and lipid metabolism in pigs. *J Virol* **85**, 11626-11637 (2011). https://doi.org:10.1128/JVI.05705-11

15 Reed, L. J. & Muench, H. A Simple Method of Estimating Fifty Per Cent Endpoints12. *American Journal of Epidemiology* **27**, 493-497 (1938). https://doi.org:10.1093/oxfordjournals.aje.a118408

16 Gaudreault, N. N. *et al.* SARS-CoV-2 infection, disease and transmission in domestic cats. *Emerg Microbes Infect* **9**, 2322–2332 (2020). https://doi.org:10.1080/22221751.2020.1833687

17 Sponseller, B. A. *et al.* Influenza A pandemic (H1N1) 2009 virus infection in domestic cat. *Emerg Infect Dis* **16**, 534-537 (2010). https://doi.org:10.3201/eid1603.091737

18 Gauger, P. C. & Vincent, A. L. Serum Virus Neutralization Assay for Detection and Quantitation of Serum Neutralizing Antibodies to Influenza A Virus in Swine. *Methods Mol Biol* **2123**, 321-333 (2020). https://doi.org:10.1007/978-1-0716-0346-8_23

19 Artiaga, B. L. *et al.* Evaluating alpha-galactosylceramide as an adjuvant for live attenuated influenza vaccines in pigs. *Anim Dis* **2**, 19 (2022). https://doi.org:10.1186/s44149-022-00051-x

20 Lee, J. *et al.* Effects of PB1-F2 on the pathogenicity of H1N1 swine influenza virus in mice and pigs. *J Gen Virol* **98**, 31-42 (2017). https://doi.org:10.1099/jgv.0.000695

21 Lee, D. H. Complete Genome Sequencing of Influenza A Viruses Using Next-Generation Sequencing. *Methods Mol Biol* **2123**, 69-79 (2020). https://doi.org:10.1007/978-1-0716-0346-8_6

22 Zhou, B. & Wentworth, D. E. Influenza A virus molecular virology techniques. *Methods Mol Biol* **865**, 175-192 (2012). https://doi.org:10.1007/978-1-61779-621-0_11

23 Hoffmann, E., Stech, J., Guan, Y., Webster, R. G. & Perez, D. R. Universal primer set for the full-length amplification of all influenza A viruses. *Arch Virol* **146**, 2275-2289 (2001). https://doi.org:10.1007/s007050170002

24 Mena, I. *et al.* Origins of the 2009 H1N1 influenza pandemic in swine in Mexico. *Elife* **5** (2016). https://doi.org:10.7554/eLife.16777

25 World Health Organization. Tool for Influenza Pandemic Risk Assessment (TIPRA). (2020).

26 Rajao, D. S. & Vincent, A. L. Swine as a model for influenza A virus infection and immunity. *ILAR J* **56**, 44-52 (2015). https://doi.org:10.1093/ilar/ilv002

27 Ito, T. *et al.* Molecular basis for the generation in pigs of influenza A viruses with pandemic potential. *J Virol* **72**, 7367-7373 (1998). https://doi.org:10.1128/JVI.72.9.7367-7373.1998

28 Kaplan, B. S., Torchetti, M. K., Lager, K. M., Webby, R. J. & Vincent, A. L. Absence of clinical disease and contact transmission of HPAI H5NX clade 2.3.4.4 from North America in experimentally infected pigs. *Influenza Other Respir Viruses* **11**, 464-470 (2017). https://doi.org:10.1111/irv.12463

29 Graaf, A. *et al.* Low Susceptibility of Pigs against Experimental Infection with HPAI Virus H5N1 Clade 2.3.4.4b. *Emerg Infect Dis* **29**, 1492-1495 (2023). https://doi.org:10.3201/eid2907.230296

30 Balzli, C. *et al.* Susceptibility of swine to H5 and H7 low pathogenic avian influenza viruses. *Influenza Other Respir Viruses* **10**, 346-352 (2016). https://doi.org:10.1111/irv.12386

31 Richt, J. A. *et al.* Pathogenic and antigenic properties of phylogenetically distinct reassortant H3N2 swine influenza viruses cocirculating in the United States. *J Clin Microbiol* **41**, 3198-3205 (2003). https://doi.org:10.1128/JCM.41.7.3198-3205.2003

32 Ma, W. *et al.* Identification of H2N3 influenza A viruses from swine in the United States. *Proc Natl Acad Sci U S A* **104**, 20949-20954 (2007). https://doi.org:10.1073/pnas.0710286104

33 Elsmo, E. J. *et al.* Pathology of natural infection with highly pathogenic avian influenza virus (H5N1) clade 2.3.4.4b in wild terrestrial mammals in the United States in 2022. *bioRxiv* (2023). https://doi.org:10.1101/2023.03.10.532068

34 Thorsson, E. *et al.* Highly Pathogenic Avian Influenza A(H5N1) Virus in a Harbor Porpoise, Sweden. *Emerg Infect Dis* **29**, 852-855 (2023). https://doi.org:10.3201/eid2904.221426

35 Bordes, L. *et al.* Highly Pathogenic Avian Influenza H5N1 Virus Infections in Wild Red Foxes (Vulpes vulpes) Show Neurotropism and Adaptive Virus Mutations. *Microbiol Spectr* **11**, e0286722 (2023). https://doi.org:10.1128/spectrum.02867-22

36 Kida, H. *et al.* Potential for transmission of avian influenza viruses to pigs. *J Gen Virol* **75 (Pt 9)**, 2183-2188 (1994). https://doi.org:10.1099/0022-1317-75-9-2183

37 De Vleeschauwer, A., Van Poucke, S., Braeckmans, D., Van Doorsselaere, J. & Van Reeth, K. Efficient transmission of swine-adapted but not wholly avian influenza viruses among pigs and from pigs to ferrets. *J Infect Dis* **200**, 1884-1892 (2009). https://doi.org:10.1086/648475

38 Shortridge, K. F. *et al.* Characterization of avian H5N1 influenza viruses from poultry in Hong Kong. *Virology* **252**, 331-342 (1998). https://doi.org:10.1006/viro.1998.9488

39 Choi, Y. K. *et al.* Studies of H5N1 influenza virus infection of pigs by using viruses isolated in Vietnam and Thailand in 2004. *J Virol* **79**, 10821-10825 (2005). https://doi.org:10.1128/JVI.79.16.10821-10825.2005

40 Maemura, T. *et al.* Characterization of highly pathogenic clade 2.3.4.4b H5N1 mink influenza viruses. *EBioMedicine* **97**, 104827 (2023). https://doi.org:10.1016/j.ebiom.2023.104827

41 Lee, J. H. *et al.* Isolation and genetic characterization of H5N2 influenza viruses from pigs in Korea. *J Virol* **83**, 4205-4215 (2009). https://doi.org:10.1128/JVI.02403-09

548 42 Bussey, K. A., Bousse, T. L., Desmet, E. A., Kim, B. & Takimoto, T. PB2 residue 271 plays a key role
549 in enhanced polymerase activity of influenza A viruses in mammalian host cells. *J Virol* **84**, 4395-
550 4406 (2010). https://doi.org:10.1128/JVI.02642-09
551 43 Neumann, G., Chen, H., Gao, G. F., Shu, Y. & Kawaoka, Y. H5N1 influenza viruses: outbreaks and
552 biological properties. *Cell Res* **20**, 51-61 (2010). https://doi.org:10.1038/cr.2009.124
553 44 Kim, J. H. *et al.* Role of host-specific amino acids in the pathogenicity of avian H5N1 influenza
554 viruses in mice. *Journal of General Virology* **91**, 1284-1289 (2009).
555 https://doi.org:10.1099/vir.0.018143-0
556 45 Herfst, S. *et al.* Airborne transmission of influenza A/H5N1 virus between ferrets. *Science* **336**,
557 1534-1541 (2012). https://doi.org:10.1126/science.1213362
558 46 Linster, M. *et al.* Identification, characterization, and natural selection of mutations driving
559 airborne transmission of A/H5N1 virus. *Cell* **157**, 329-339 (2014).
560 https://doi.org:10.1016/j.cell.2014.02.040
561 47 Hatta, M., Gao, P., Halfmann, P. & Kawaoka, Y. Molecular Basis for High Virulence of Hong Kong
562 H5N1 Influenza A Viruses. *Science* **293**, 1840-1842 (2001).
563 https://doi.org:10.1126/science.1062882
564 48 Steel, J., Lowen, A. C., Mubareka, S. & Palese, P. Transmission of influenza virus in a mammalian
565 host is increased by PB2 amino acids 627K or 627E/701N. *PLoS Pathog* **5**, e1000252 (2009).
566 https://doi.org:10.1371/journal.ppat.1000252
567 49 Taft, A. S. *et al.* Identification of mammalian-adapting mutations in the polymerase complex of
568 an avian H5N1 influenza virus. *Nat Commun* **6**, 7491 (2015).
569 https://doi.org:10.1038/ncomms8491
570 50 Song, W. *et al.* The K526R substitution in viral protein PB2 enhances the effects of E627K on
571 influenza virus replication. *Nat Commun* **5**, 5509 (2014). https://doi.org:10.1038/ncomms6509
572 51 Stevens, J. *et al.* Structure and receptor specificity of the hemagglutinin from an H5N1 influenza
573 virus. *Science* **312**, 404-410 (2006). https://doi.org:10.1126/science.1124513
574 52 Lindh, E. *et al.* Highly pathogenic avian influenza A(H5N1) virus infection on multiple fur farms in
575 the South and Central Ostrobothnia regions of Finland, July 2023. *Euro Surveill* **28** (2023).
576 https://doi.org:10.2807/1560-7917.ES.2023.28.31.2300400
577 53 Adlhoch, C. *et al.* Avian influenza overview April - June 2023. *EFSA J* **21**, e08191 (2023).
578 https://doi.org:10.2903/j.efsa.2023.8191

579

580 **Acknowledgments**

581 We gratefully thank Yonghai Li, Patricia Assato, Michelle Zajac, Isaac Fitz for technical assistance, and
582 Innovative Diagnostics for providing ELISA kits. Funding for this study was provided through grants
583 from the NIAID supported Center of Excellence for Influenza Research and Response (CEIRR) under
584 contract number 75N93021C00016, the National Bio and Agro-Defense Facility (NBAF) Transition Fund
585 from the State of Kansas, the MCB Core of the Center on Emerging and Zoonotic Infectious Diseases
586 (CEZID) of the National Institutes of General Medical Sciences under award number P20GM130448, the

NIAID Centers of Excellence for Influenza Research and Surveillance (CEIRS) under contract number HHSN 272201400006C.

Author contributions

J.A.R and N.O. conceptualized the research project. T.K., J.D.T., M.C., E.L.L., C.D.M., K.C., F.S.M., T.J., I.M., N.N.G., U.B.R.B., N.O., R.J.W. and J.A.R acquired the data.

Competing interests

The J.A.R. laboratory received support from Tonix Pharmaceuticals, Genus *plc*, Xing Technologies, and Zoetis, outside of the reported work. J.A.R. is inventor on patents and patent applications on the use of antivirals and vaccines for the treatment and prevention of virus infections, owned by Kansas State University. The other authors declare no competing interests.

601 **Figure legions**

602 **Figure 1.** Infection with a mink-derived clade 2.3.4.4b H5N1 isolate in pigs. **A** The pigs (n=9) were
603 orally, intra-nasally, and intra-tracheally infected with 2.2×10^7 $TCID_{50}$ of A/Mink/Spain/3691-
604 8_22VIR10586-10/2022 and sentinel pigs (n=6) were introduced in a same pen at 2 days post-challenge
605 (DPC). Swab and serum samples were collected throughout the study. Principal infected pigs were
606 euthanized and necropsied at 3 and 5 DPC (n=3 per time point) and the remaining three principals and 6
607 sentinels were euthanized and necropsied at 21 DPC. **B** Infectious virus titers in bronchoalveolar lavage
608 fluids at 3 and 5 DPC and **C and D** infectious virus titers in tissues at (C) 3 DPC and (D) 5 DPC. **E and F**
609 Antibody responses were evaluated in three principal pigs at -1, 7, 14, and 21 DPC. Virus neutralization
610 (VN) titers (E) were a reciprocal of the highest serum dilution inhibiting replication of the homologous
611 H5N1 virus. ELISA antibody titers were calculated in a swine indirect ELISA kit (ID Screen® Influenza
612 A Nucleoprotein Swine Indirect, Innovative Diagnostics, France) where S/P ratios were calculated from
613 O.D. values and then converted to antibody titers according to the manufacturers' instruction. Dash lines
614 represent the limit of detection of each assay (the limit of detection of each assay (4.64×10^1 $TCID_{50}$/mL
615 for BALF titration, 2.92×10^1 $TCID_{50}$/mL for tissue titration, 1:10 for VN assay, and 1053 for ELISA
616 antibody titer). Empty circle represents negative results in each assay.

617

618 **Figure 2.** Macroscopic and microscopic lung scores in a mink-derived clade 2.3.4.4b H5N1 virus-
619 infected pigs. Infected pigs were euthanized at 3, 5, and 21 DPC for pathological evaluation. Macroscopic
620 lung scores were determined by the percentage of the surface area showing IAV-induced pneumonia.
621 Microscopic scores were calculated by the average of six different criteria (see Materials and Methods)

622

623 **Figure 3.** Histological features and tropism of mink-derived H5N1 clade 2.3.4.4b influenza virus in pigs.
624 Histologically, pulmonary lesions were characterized by necrotizing to lymphohistiocytic

625 bronchointerstitial pneumonia. At 3 DPC (A and B), multifocal bronchopulmonary segments were
626 characterized by bronchiolar epithelial cell necrosis (A, inset 1) and associated areas of pulmonary
627 parenchyma with expanded alveolar septa infiltrated by lymphocytes and histiocytes and alveolar
628 epithelial necrosis (A, inset 2). Influenza A virus NP intracytoplasmic antigen was detected within
629 bronchiolar epithelial cells (B, asterisk), pneumocytes and alveolar macrophages (B, inset). Intranuclear
630 viral antigen was typically detected within infected epithelial cells. Similar but more extensive and severe
631 histological changes were noted at 5 DPC (C and D), with similar alveolar (C, inset 1) and bronchiolar (C,
632 inset 2) alterations. Influenza A virus NP antigen was more abundant but had a similar cellular distribution
633 compared to 3 DPC (D and insets 1 and 2). At 21 DPC, the airway epithelia had mostly repaired but
634 multifocal areas of interstitial inflammation persisted (E, inset). Only sporadic epithelial cells contained
635 viral antigen at this timepoint (F and insets).

636 **Figure 4.** Detection of mink-derived H5N1 clade 2.3.4.4b influenza virus RNA via in situ hybridization
637 (ISH). Probes specific to the NP and HA (H5) genes were designed. Viral RNA was predominantly
638 detected within bronchiolar epithelial cells and intraluminal cellular debris at 3 (A and B) and 5 DPC (C
639 and D). RNAscope® ISH, Fast Red, total magnification 200X.

640

641

642

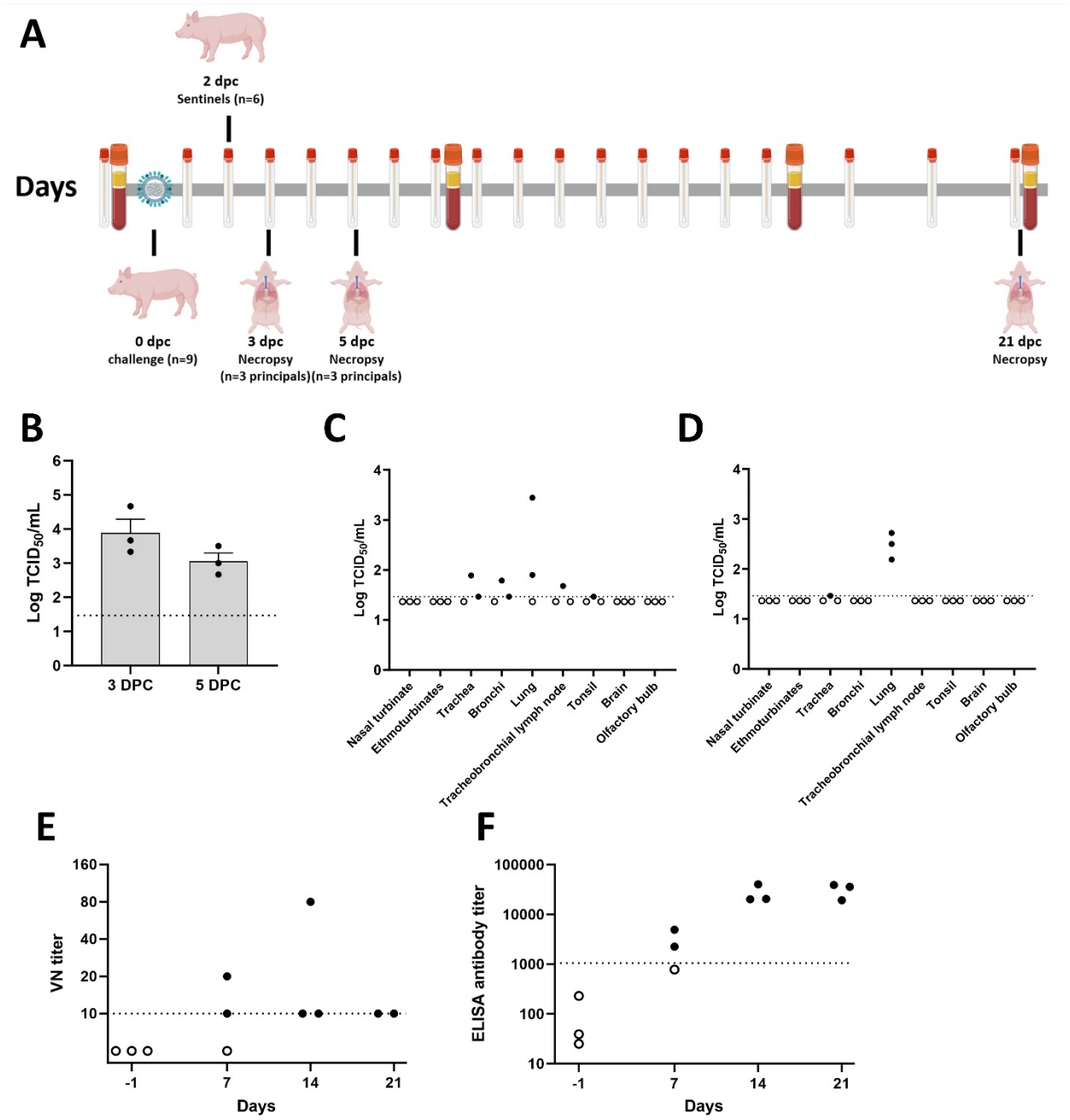
A
2 dpc
Sentinels (n=6)
Days
0 dpc
challenge (n=9)
3 dpc
Necropsy
(n=3 principals)
5 dpc
Necropsy
(n=3 principals)
21 dpc
Necropsy
B
Log TCID50/mL
3 DPC
5 DPC
C
Log TCID50/mL
Nasal turbinate
Ethmoturbinates
Trachea
Bronchi
Lung
Tracheobronchial lymph node
Tonsil
Brain
Olfactory bulb
D
Log TCID50/mL
E
VN titer
Days
F
ELISA antibody titer
Days

Figure 1

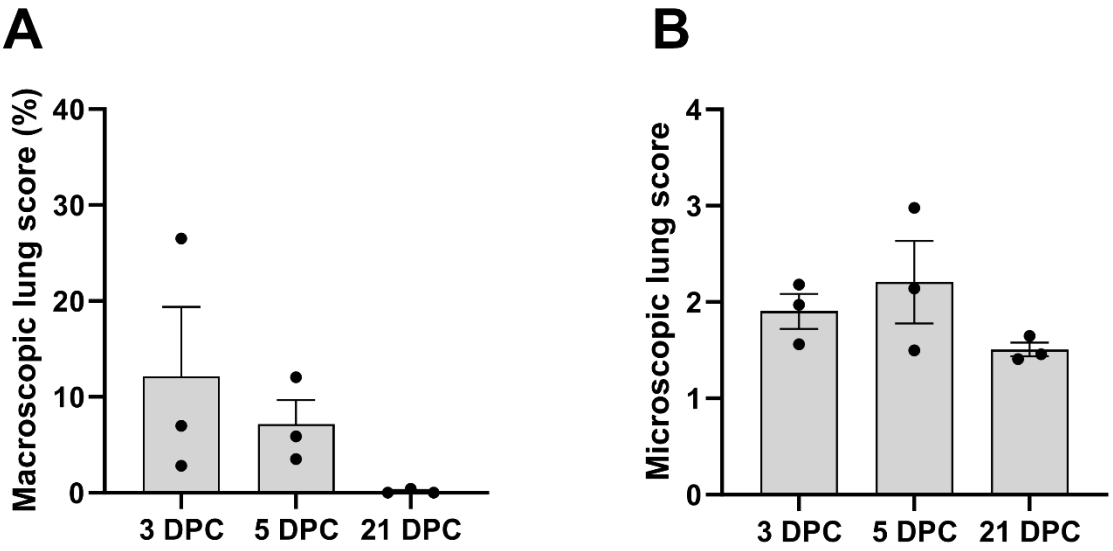
A
Macroscopic lung score (%)
40
30
20
10
0
3 DPC
5 DPC
21 DPC
B
Microscopic lung score
4
3
2
1
0
3 DPC
5 DPC
21 DPC

Figure 2.

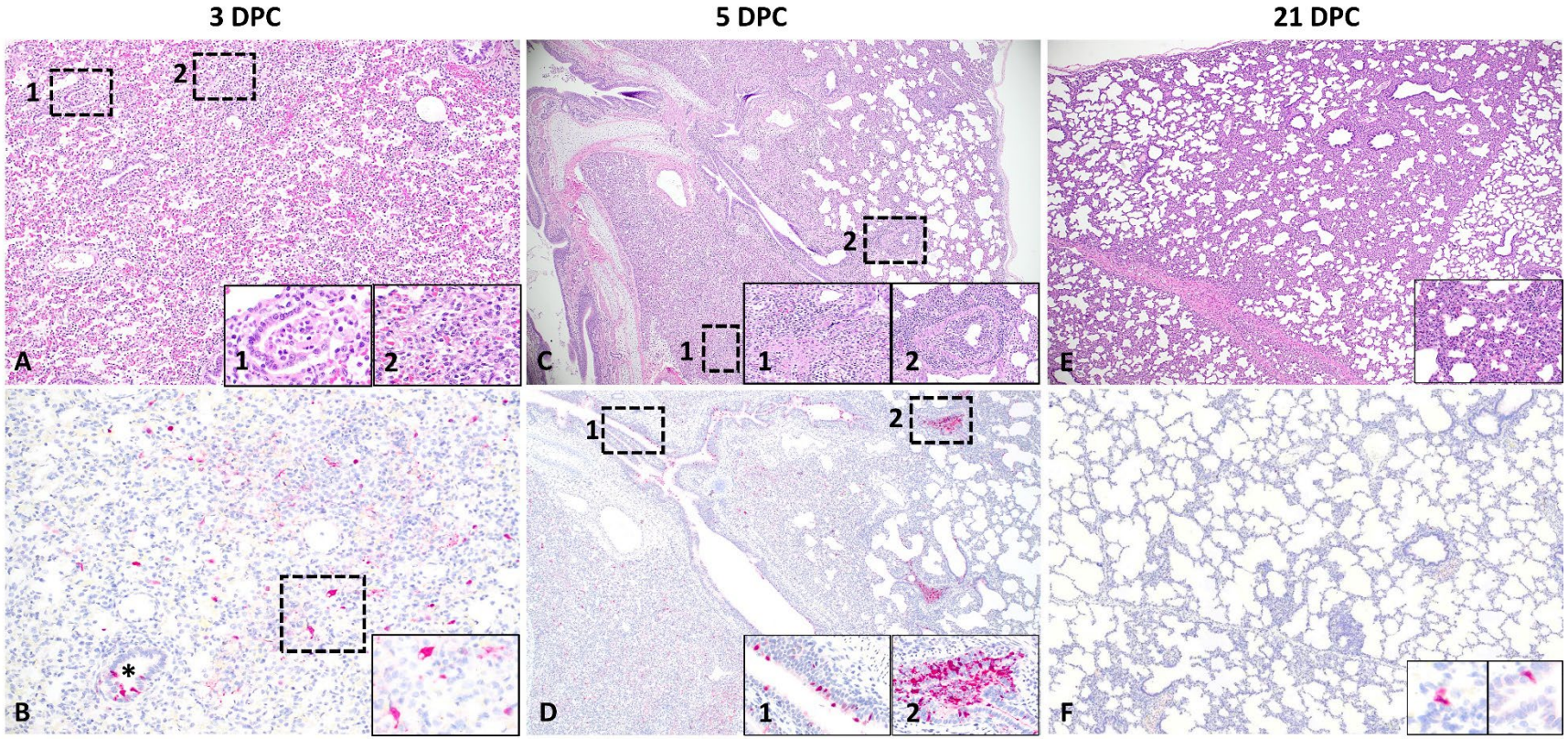

647

648 **Figure 3.**

649

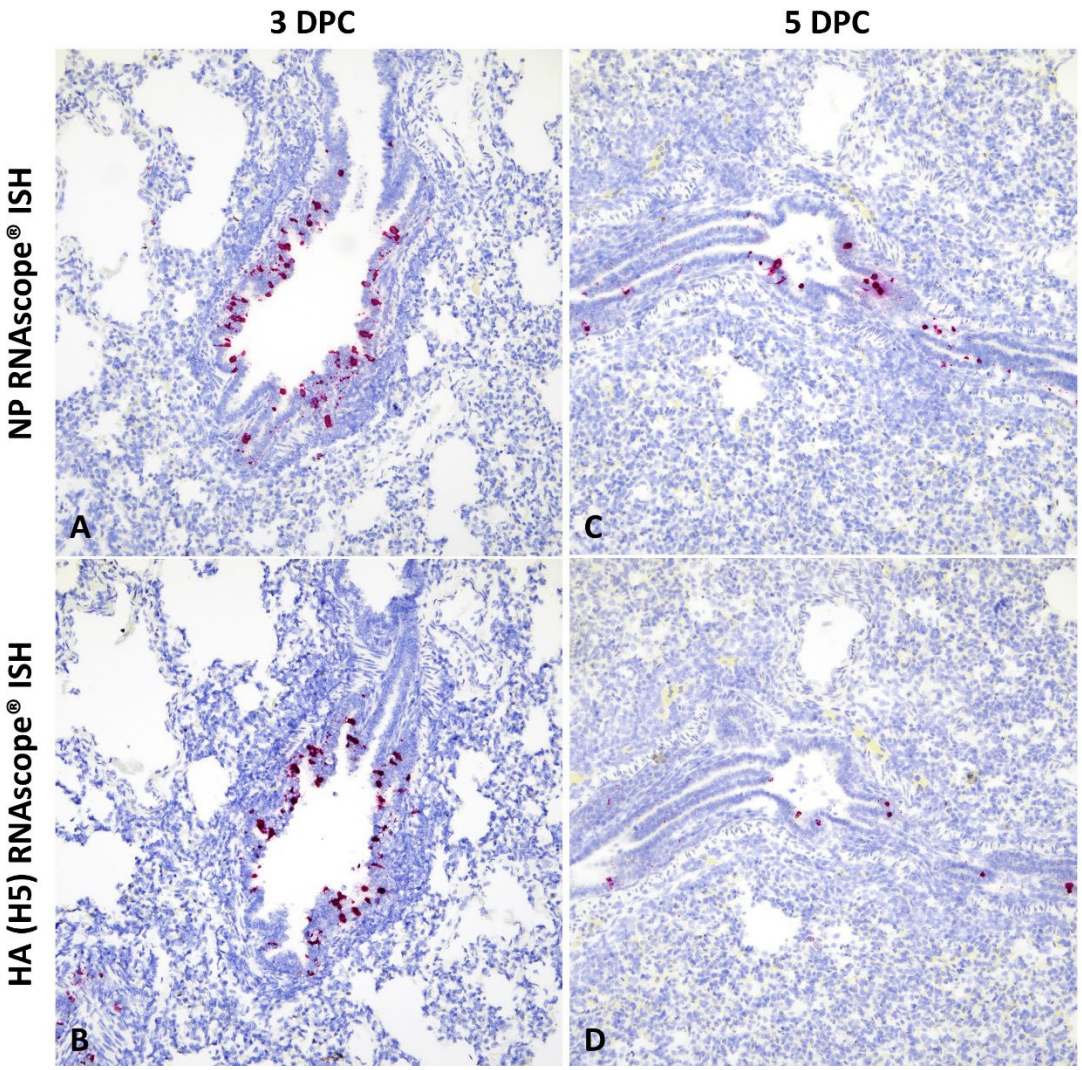

Figure 4.

652 **Table 1.** Virus shedding in pigs infected with the mink-derived clade 2.3.4.4b H5N1 virus.

Days post-challenge (DPC)			1	2	3	4	5	6 to 21[a]
Nasal swab	Principal	# of positive / # of animals	6/9	0/9	1/9	0/6	1/6	0/3
		Virus titer ($TCID_{50}$/mL)	4.6×10^{1} to 1×10^{3}	Neg	2.15×10^{3}	Neg	2.15×10^{2}	Neg
	Sentinel	# of positive / # of animals	0/6	0/6	0/6	0/6	0/6	0/6
Oropharyngeal swab	Principal	# of positive / # of animals	4/9	N/A[b]	1/9	N/A[b]	0/6	0/3
		Virus titer ($TCID_{50}$/mL)	1×10^{2} to 4.6×10^{2}	N/A[b]	4.6×10^{2}	N/A[b]	Neg	Neg
	Sentinel	# of positive / # of animals	0/6	N/A[b]	0/6	N/A[b]	0/6	0/6

653 [a]Nasal swabs were collected at 6 to 14, 17 and 21 DPC and oropharyngeal swabs were at 7, 10, 14, 17,

654 and 21 DPC. [b]N/A: Samples were not collected.

655

Table 2. Mammalian-like adaptive mutations after replication of a mink-derived clade 2.3.4.4b H5N1 in pigs.

Viral protein	Amino acid substitution	Inoculum	Nasal swab, #517, 1 DPC	Nasal swab, #517, 3 DPC	OP swab, #94, 1 DPC	OP swab, #517, 1 DPC	OP swab, #571, 1 DPC	OP swab, #839, 1 DPC	OP swab, #634, 3 DPC	BALF, #517, 3 DPC	BALF, #575, 3 DPC	BALF, #839, 3 DPC	BALF, #94, 5 DPC	BALF, #213, 5 DPC	BALF, #714, 5 DPC
PB2 [a]	K526R	< 2%	< 2%	< 2%	< 2%	**3.14%**	< 2%	< 2%	< 2%	< 2%	< 2%	< 2%	< 2%	< 2%	< 2%
	E627K	< 2%	< 2%	< 2%	< 2%	< 2%	**4.71%**	< 2%	< 2%	< 2%	< 2%	**5.19%**	< 2%	< 2%	< 2%
	E627V	< 2%	< 2%	< 2%	**6.96%**	< 2%	< 2%	< 2%	< 2%	< 2%	< 2%	< 2%	< 2%	**2.02%**	< 2%
HA	Q222L	< 2%	< 2%	< 2%	**2.10%**	< 2%	< 2%	< 2%	< 2%	< 2%	< 2%	< 2%	< 2%	< 2%	< 2%

[a] Amino acid substitution with a frequency >2% was not found at position of 271 of PB2 in all samples tested.

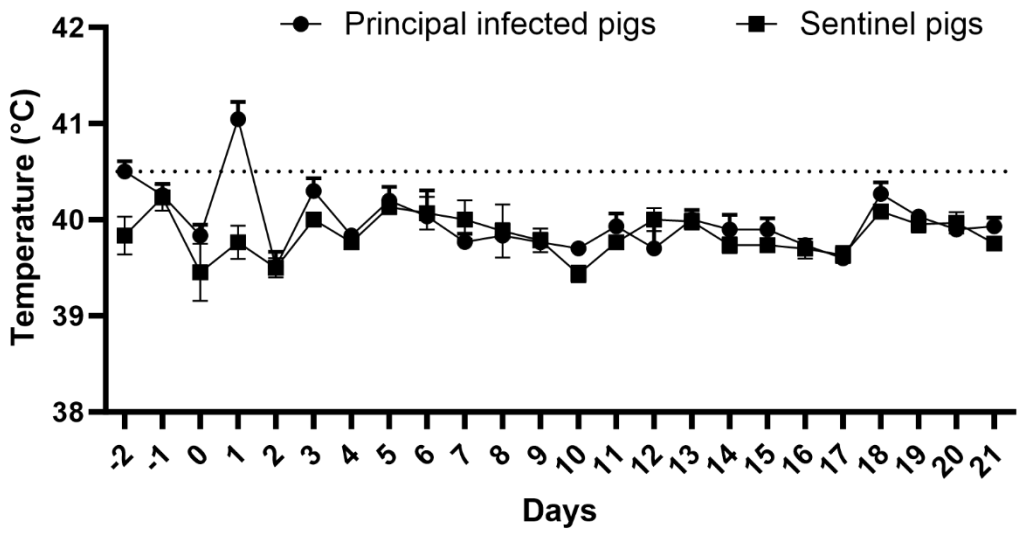

Supplementary Figure 1. Daily body temperature of principal infected and sentinels in this study. The value is expressed as the mean ± SEM. The dash line indicates 40.5 °C, which is considered fever in this study.

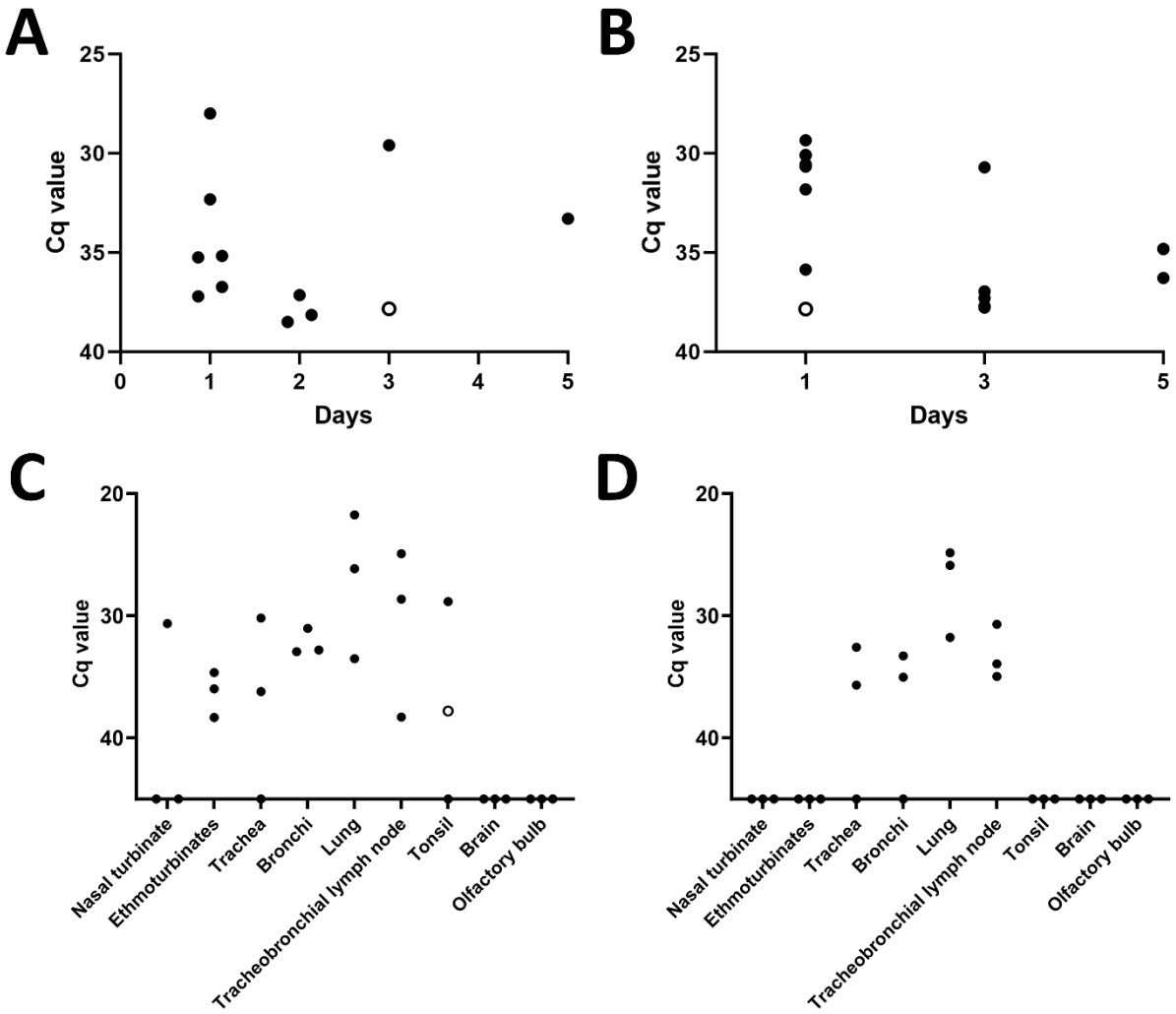

Supplementary Figure 2. Viral RNA detection in (A) nasal swab and (B) oropharyngeal swab of H5N1-infected pigs (n=9, at 1, 2, and 3 days post-challenge (DPC); and n=6, at 4 and 5 DPC). The Cq values of positive swabs were shown in the graphs. The distribution of viral RNA in tissues of H5N1-infected pigs at (C) 3 DPC and (D) 5 DPC. Empty circles represent the single well positive in duplicates.

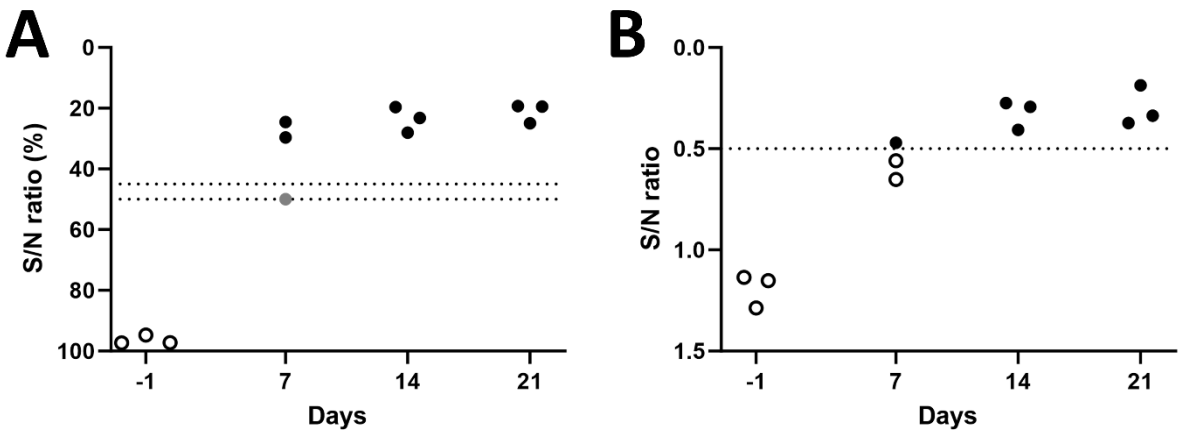

Supplementary Figure 3. Antibody responses in H5N1-infected pigs employing two competitive ELISAs: (A) ID Screen® Influenza A Antibody Competition Multi-Species and (B) IDEXX AI MultiS-Screen Ab Test. Empty and grey circles represent negative and suspicious.

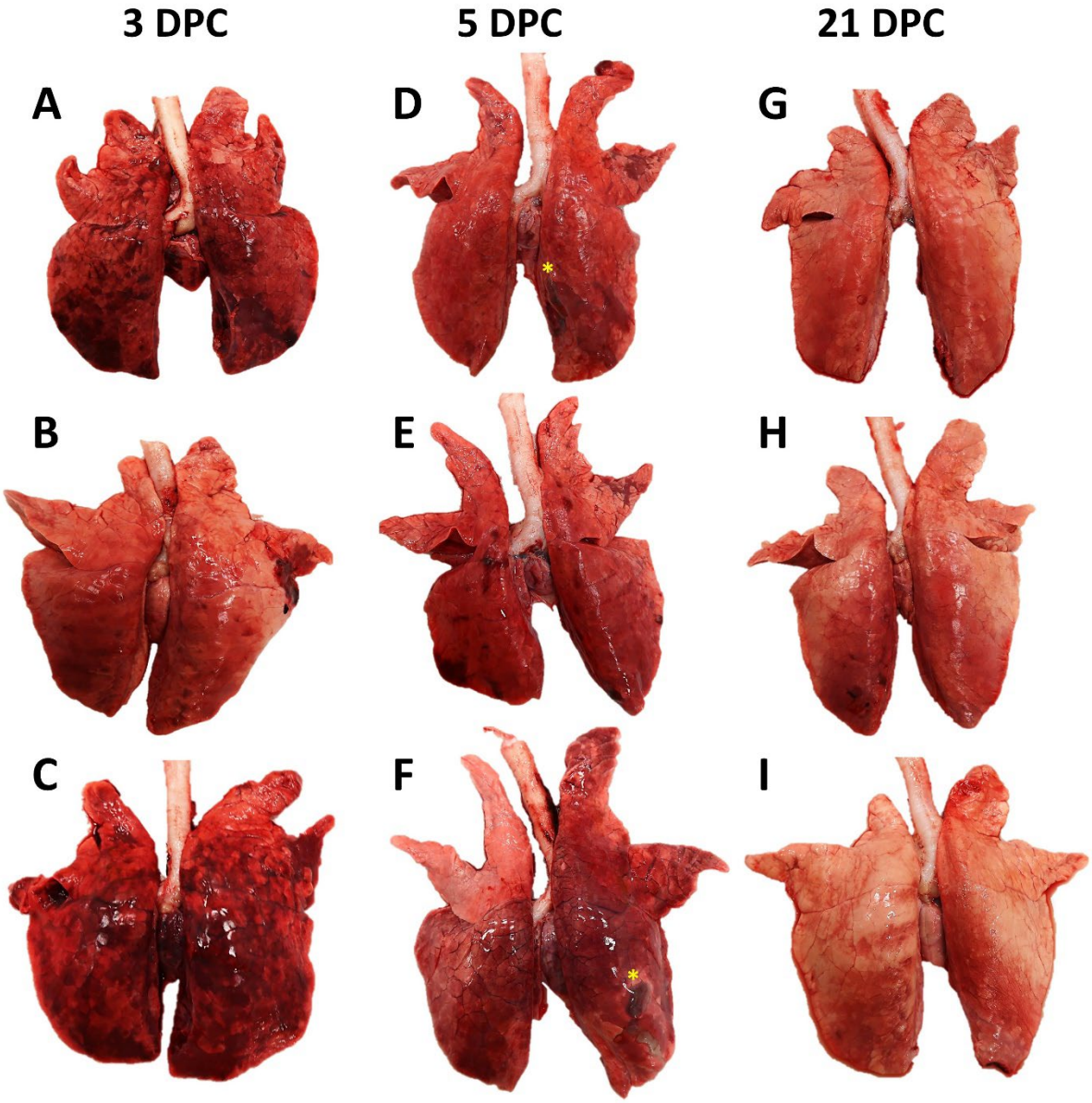

Supplementary Figure 4. Gross changes in the lungs of a mink-derived clade 2.3.4.4b H5N1 virus-infected pigs at 3, 5 and 21 DPC. At 3 DPC, two pigs (A and B) had moderate to severe, multifocal to coalescing interstitial pneumonia with congestion and edema affecting all lobes (A and B), while the third animal (C) had mild, multifocal pneumonia with congestion affecting predominately the right lung and left caudal lung lobes (C). At 5 DPC (D–F), coalescing areas of pulmonary consolidation with congestion and edema were noted in all pigs. The right middle and caudal lobes were most commonly affected (D–F) with occasional bullae (asterisk). At 21 DPC, only a few areas of pulmonary consolidation were noted (G–I).

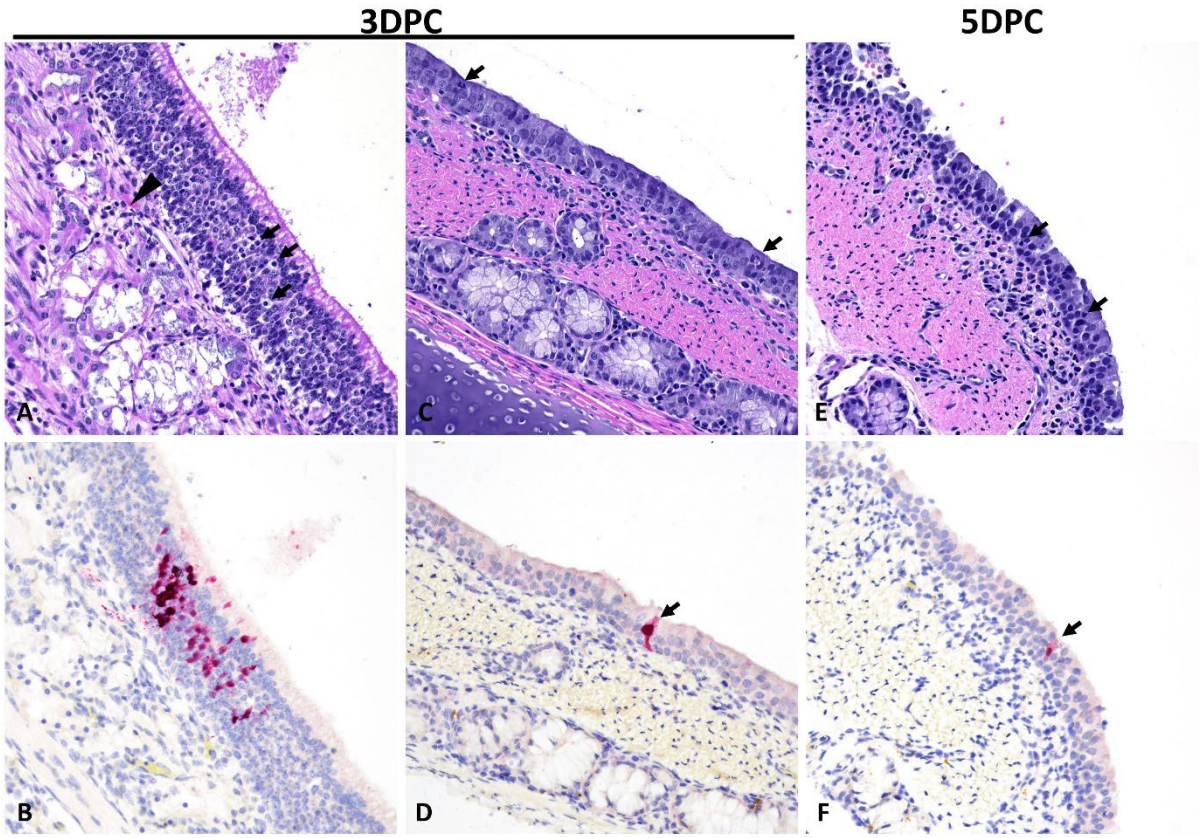

Supplementary Figure 5. Histological and immunohistochemical findings in the upper respiratory tract of pigs infected with a mink-derived clade 2.3.4.4b H5N1 virus. In a single animal, a focal area of the olfactory epithelium is mildly infiltrated by few lymphocytes (A, arrows) that also mildly infiltrate the subjacent lamina propria (A, arrowhead) at 3 DPC. Within this area, olfactory epithelia contain abundant influenza NP antigen (B, intracytoplasmic and intranuclear). At 3 and 5 DPC, there is mild lymphohistiocytic and neutrophilic tracheitis (C and E) with lymphocytes and histiocytes within the lamina propria and sporadic neutrophils and lymphocytes transmigrating through the lining epithelium (arrows). Sporadic epithelial cells contain intracytoplasmic and intranuclear influenza NP antigen (D and F, arrows). H&E (A, C, E) and IHC (Fast Red, B, D and F), total magnification 200X.

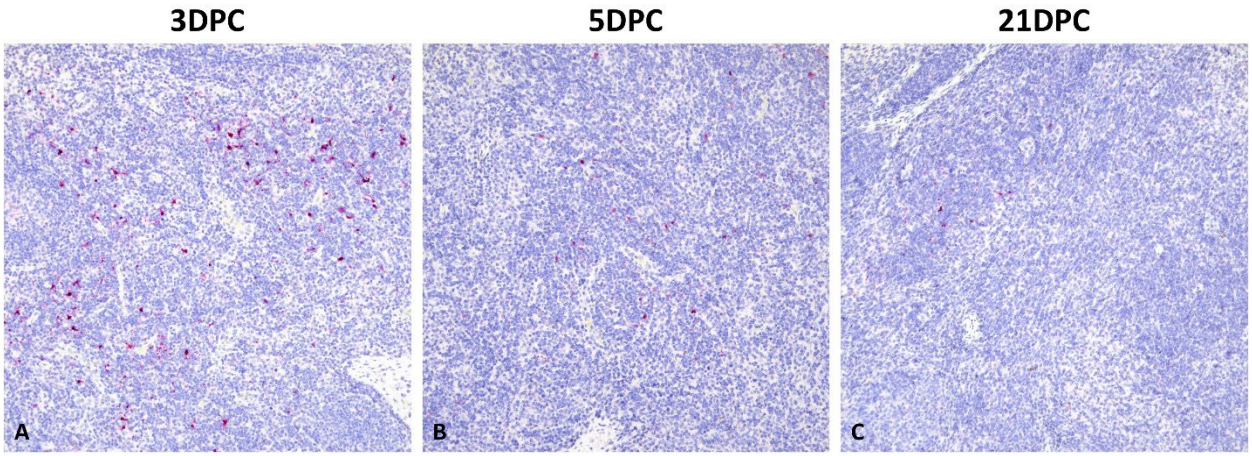

Supplementary Figure 6. Immunohistochemical findings in the tracheobronchial lymph nodes of pigs infected with a mink-derived clade 2.3.4.4b H5N1 virus. At 3 DPC (A), there are numerous influenza NP antigen-positive cells with dendritic projections of their cytoplasm (consistent with antigen presenting cells). The number of immune-positive cells gradually declines at 5 and 21 DPC (B and C, respectively). IHC, Fast Red, total magnification 100X.

Supplementary Table 2. Frequencies of mutations of a mink-derived clade 2.3.4.4b H5N1 in pigs. Blank represents less than 2%.

Viral protein	Amino acid substitution	Inoculum	Nasal swab, #517, 1 DPC	Nasal swab, #517, 3 DPC	OP swab, #94, 1 DPC	OP swab, #517, 1 DPC	OP swab, #571, 1 DPC	OP swab, #839, 1 DPC	OP swab, #634, 3 DPC	BALF, #517, 3 DPC	BALF, #575, 3 DPC	BALF, #839, 3 DPC	BALF, #94, 5 DPC	BALF, #213, 5 DPC	BALF, #714, 5 DPC
PB2	R70W														3.35
	K80R								9.67						
	R101G											3.47			
	P104T							3.25							
	N137K		6.95												
	K140E								2.70						
	V167I												2.57		
	P169S											2.25			
	E180G														9.86
	E188G					2.47									
	D195N		3.28		7.01				3.43						
	V220I												2.49		
	T238A											2.28			
	C239Y													3.71	
	M243K	2.68													
	T245A			3.64											
	R269G														8.89
	S279L						2.12								
	S286N						4.70								
	L317S													2.52	
	N348S												3.04		
	E396K										2.22				
	F420L														2.80
	M431T													2.06	
	H437R			3.91											
	K440R				7.25										
	I463M							3.04							
	S474P												3.00		
	M483K	2.43													
	S497G	2.67													
	K526R					3.14									
	D611N											4.03	2.35		
	T612A					6.26	2.11				2.37		3.95		
	L618I				3.83										
	E627K						4.71					5.19			
	E627V				6.96									2.02	
	R641G								4.29						
	M645V		2.37		4.09	2.80	2.76	5.20		2.57			2.08	20.07	
	Y658C	2.50													
	E681K											2.80			
	G682E									3.30					
	L691S										2.24				

	R703K		4.87			2.04									
	S709G					2.11									
	A717T									2.31					
	K721R											4.53			
	D740N				6.17										
	A750S														3.19
PB1	K11E							10.49							
	T36A														3.32
	M40T														2.49
	Q48K											2.06			
	A91T					3.89									
	G101W											3.43			
	T123A													2.01	
	Y129C											2.65			
	P138T										3.10				
	M171V								2.10				16.58		
	M174T										4.14				
	V191I											3.18			
	R192K				3.45										
	K207R													3.19	
	K209R											5.92			
	A221T														4.85
	I248V													4.47	
	G250R									3.02					
	S261G							2.51							
	V273I					2.21							3.28		
	E277G			4.14											
	N292D												2.84		
	Q313R				7.01										
	P315S									4.91					
	A320T							2.79							
	I322T													2.49	
	V336A												4.64		
	A340S	2.63													
	A349V							2.78							
	D377N								2.22						
	K387E	2.50													
	K387R		3.80												
	L424P													2.06	
	I450R												3.53		
	D464G								5.79						
	I475V			4.10											
	M546V														2.11
	A547V											2.17			
	L598P										3.69				
	P607S							2.39							
	L611S												3.11		
	L628P			4.88											

	N641S												2.92		
	V644A														3.09
	V660I	31.83	60.36	78.21	33.58	19.61	31.99	19.32	16.78	22.83	15.91	16.95	4.59	13.76	10.24
	C692R			10.62											
	I711V								3.32						
	K745R				2.18										
PA	F4L												2.17		
	F9L												3.40		
	K19R							2.02							
	F46S				2.72						3.63				
	S65P								5.15						
	V100A													5.69	
	K113R							3.37							
	F117S				3.65										
	K139R				2.80										
	H146Q				5.08										
	F150L					3.52						15.63			
	Y161C										2.27				
	T162A		18.72												
	E198K		2.09												
	K245E			25.03											
	L246P			6.31											
	N254D														2.13
	R266Q												4.00		
	D272N		2.66												
	K318R												3.48		
	V323A										2.25				
	N331D		2.12												
	Q340K									3.46					
	D352N													9.70	
	K358R												5.97		
	D380Y				2.14										
	D394N													9.01	
	R401K											3.36			
	L425F		4.06	63.88				2.32							
	E427K					4.25									
	A433T													3.97	
	M441R										5.50				
	K461R												4.38		
	F480L					3.86									
	M485I												3.17		
	N499T												5.48		
	H510R														12.57
	E538K	5.95								4.13			6.50	6.06	
	E538G		3.34	59.10											
	G578S														12.95
	L589R								2.50						
	E599G											2.08			

	E623G				2.73										
	S632P								5.48						
	S632F									3.63					
	V645A							2.16							
	F681L			13.38											
	E688K							3.47							
	N696D													4.89	
	L711F													4.70	
HA	Q2R					2.13									
	E14G			2.62											
	V16I											3.79			
	H28Y		8.19												
	V57I														2.31
	D68G							5.25							
	V80A							6.22							
	L101M		3.39												
	A140V										2.29	3.69			
	S142F		4.12												
	I151V													6.59	
	K152E													3.86	
	D155N													6.92	
	I174M											2.01			
	N183D							5.81							
	L190I												8.85		
	T202R											4.49			
	Q207Stop		2.23												
	Q222L			2.10											
	M289V		2.98												
	C302R											2.57			
	Y305F								3.23						
	K310R								3.40						
	V312I		22.45					30.67							
	L322P											2.70			
	R327K										2.45				
	G341E													4.43	
	M374I		15.49		3.76			68.45					2.52	8.03	
	M413I													6.69	
	D419Y									2.70					
	V481A												2.09		
	N483S							2.19							
	I510V													9.45	3.12
NP	I57V		5.04												
	G86E				5.33										
	V105A							2.10							
	R156H													8.67	
	A181V														7.39
	D290N						3.17								
	F338S		3.75												

	S344T											3.47	2.20		
	S402P													5.72	
	V408I													6.53	
NA	T10I				4.89				5.28						
	H36R													3.28	
	N73I		2.16												
	Q78L		3.87												
	S82L										2.48				
	V83A						2.05								
	N104S				2.94										
	L134P												2.51		
	L140P		2.39												
	P162L													11.73	
	A178D											3.61			
	I188V											2.51			
	G236S														15.58
	S237P										2.44				
	V264A												2.29		
	V304I										2.75				
	Y353Stop														2.05
	E372K			11.12											
	D376G													2.24	
	T381N													4.87	
	M396I												5.12		
M1	V15I											5.21			
	A25T													4.37	
	M43I		3.16												
	I59V			2.62											
	L103S				2.03										
	G220R														5.97
M2	S20N												2.36		
	L40S			3.05											
	T65K														2.79
	R77Q														2.31
	S82N									2.17					
NS1	G70D										2.00				
	M79V					2.23	2.86	2.81					15.39		3.88
	D189Y													19.15	
	Q220R					3.87				2.73	2.14		2.35	3.22	2.06
	L222R				2.18										
	Stop231W					2.13	4.64	3.00	2.58	3.44	2.17		17.38	3.74	6.73
	N29S							3.23							
NEP	M31I													19.15	
	R63G					3.87				2.73	2.14		2.35	3.22	2.06
	W65G				2.18										
	E74K													2.23	
	E74G					2.13	4.64	3.00	2.58	3.44	2.17		17.38	3.74	6.73
	K88M				2.28										